CHEMMEDCHEM
Chemistry & Drug Discovery

Supporting Information

Targeting of a Helix-Loop-Helix Transcriptional Regulator by a Short Helical Peptide

Cornelia Roschger[+],[a] Saskia Neukirchen[+],[a, b] Brigitta Elsässer,[a] Mario Schubert,[a] Nicole Maeding,[c] Thomas Verwanger,[c] Barbara Krammer,[c] and Chiara Cabrele*[a]

cmdc_201700305_sm_miscellaneous_information.pdf

Table of contents

1. Materials and methods

1.1. Materials

Peptide synthesis and analytics. Chemical reagents and solvents used for the peptide syntheses were of peptide-synthesis grade; solvents used for HPLC and spectroscopy were of HPLC or spectroscopy grade. Fmoc-protected amino acids, Rink-amide MBHA resin (loading 0.45 mmol/g), 2-(1H-benzotriazole-1-yl)-1,1,3,3-tetramethyluronium hexafluorophosphate (HBTU), 3-(diethoxyphosphoryloxy)-1,2,3-benzotriazin-4(3H)-one (DEPBT), ethyl cyano(hydroxyimino)acetate (Oxyma Pure), N,N'-diisopropylcarbodiimide (DIC), N,N-diisopropylethylamine (DIPEA), piperidine, N,N-dimethylformamide (DMF), N-methyl-2-pyrrolidinone (NMP), dichloromethane (DCM), diethylether, CH_3CN, trifluoroacetic acid (TFA) were purchased from Novabiochem (Merck Millipore, Germany), Biosolve (The Netherland) and Iris Biotech (Germany). 5(6)-Carboxyfluorescein (FAM) was purchased from Fluka. Triisopropylsilane (TIS), 1,2-ethanedithiol (EDT), thioanisole (TIA), N-hydroxybenzotriazole (HOBt), acetic anhydride, $PhSiH_3$, $Pd(PPh_3)_4$, 2,2,2-trifluoroethanol (TFE), dimethylsulfoxide (DMSO) and trypsin singles proteomics grade were purchased from Sigma-Aldrich (Germany). α-Cyano-4-hydroxycinnamic acid was purchased from Acros Organics (Germany). D_2O was from Deutero GmbH (Germany).

Protein expression. The pET22b(+) vector was purchased from Novagen. FastBreak™ cell lysis reagent was purchased from Promega. *Echerichia coli* BL21 (DE3) chemically competent cells, isopropyl-β-D-thiogalactopyranoside (IPTG), deoxyribonuclease I (DNase I) from bovine pancreas, triton X-100, phenylmethylsulfonyl fluoride (PMSF), (ethylenedinitrilo)tetraacetic acid (EDTA), sodium chloride, 2-amino-2-(hydroxymethyl)-1,3-propanediol hydrochloride (TRIS-HCl) and urea were purchased from Sigma-Aldrich. Potassium phosphate monobasic was purchased from Fluka. Lysozyme was purchased from Appli Chem. β-Mercaptoethanol was purchased from Biorad.

Molecular and cell biology. Dulbecco's modified Eagle's medium (DMEM)–high glucose, Roswell Park Memorial Institute 1640 medium (RPMI-1640), fetal bovine serum (FBS), penicilin-streptomycin, Accutase® solution, trypsin-EDTA solution, RNase, propidium iodide (PI), phosphate buffer saline (PBS), thiazolyl blue tetrazolium bromide (MTT), 5(6)-carboxyfluorescein diacetate N-succinimidyl ester (CFSE), non-essential amino acids and dimethylsulfoxide (DMSO) were purchased from Sigma-Aldrich. 3,3'-Dihexyloxacarbocyanine iodide ($DiOC_6$) was purchased from Thermo Fisher Scientific. L-Glutamine was purchased from PAA. Hoechst 33342 was purchased from Fluka. Ethanol was purchased from Merck. The breast cancer cell line MCF-7 was a gift from Prof. Dr. Walt, University of Zurich, Switzerland, and the T47D cell line was a gift from Dr. Hauser-Kronberger, Institute of Pathology, Paracelsus Medical University, Salzburg, Austria. The T24 cell line was purchased from the Leibniz Institute DSMZ-German Collection of Microorganisms and Cell Cultures, Braunschweig, Germany. The primary human lung fibroblasts were a gift from Prof. Dr. Jutta Horejs-Höck, Department of Molecular Biology, University of Salzburg, Austria.

1.2. Methods

The solid-phase peptide syntheses were carried out on an automatic peptide synthesizer (Syro, Biotage). The analytical and semipreparative HPLC equipment was from Thermo Fisher Scientific (model Ultimate 3000). The analytical columns were from Thermo Fisher Scientific (BioBasic – 18, 250x4.6 mm, 5 µm) or Macherey Nagel (NUCLEOSIL® C-18, 250x4 mm, 5 µm), the semipreparative column was from Macherey Nagel (NUCLEOSIL® C-18, 250x10 mm, 5 µm). Protein purification was performed by gel filtration chromatography (model ICS-5000$^+$ SP, Thermo Fisher Scientific) with a Phenomenex BioSep-SEC-s2000 column (7.8x300 mm, 145 Å). MALDI-TOF mass spectra were recorded on an Autoflex mass spectrometer from Bruker Daltonics using α-cyano-4-hydroxycinnamic acid as matrix for peptides and 2,5-dihydroxybenzoic acid for the protein. The UV measurements were carried out on an Agilent Cary 60 UV-Vis spectrophotometer. The circular dichroism (CD) measurements were recorded on an Applied Photophysics Chirascan-plus CD spectrometer (United Kingdom). The binding affinity measurements on immobilized protein were carried out with a surface acoustic wave (SAW) biosensor SAM®5 blue (NanoTemper). The NMR spectra were recorded on a Bruker AVANCE III HD 600 MHz spectrometer equipped with a QXI ($^1H/^{13}C/^{15}N/^{31}P$) probe. Structure optimization, ligand interaction map and molecular dynamics simulations were carried out using MOE2015.10[1] (Amber99 force field). Stepwise molecular dynamics calculations were performed by NWChem 6.6[2]. Cell uptake of fluorescent peptides was detected on an Olympus IX70 microscope and analyzed with the Cell F software. Absorption measurements of the MTT assays were recorded using the Tecan Infinite 200M Pro microplate reader. Analysis of the cell cycle distribution, subG_1 assay, apoptosis/necrosis and proliferation assays were performed on a Becton Dickinson FACSCanto II flow cytometer and analyzed with Kaluza analysis 1.5a flow cytometry software (Beckman Coulter).

2. Peptide synthesis

The linear peptides were assembled on an automatic peptide synthesizer by using Rink-amide resin and Fmoc chemistry. The side-chain protecting groups were tBu (D, E, Y), Boc (K), alloc (K to be cyclized), allyl (D to be cyclized), Pbf (R), Trt (Q, H). The Fmoc deprotection was carried out with 25% piperidine in DMF/NMP (70:30, v/v) containing 0.125 M HOBt for 3 min and 12.5% piperidine in DMF/NMP (70:30, v/v) containing 0.063 M HOBt for 12 min. The double couplings were accomplished with the mixture Fmoc-AA-OH/HOBt/HBTU/DIPEA (4:4:4:8 equiv.) for 40 min. N-terminal acetylation was performed manually with 10 equiv. acetic anhydride and 10 equiv. DIPEA in DMF for 20 min. Alternatively, FAM (5 equiv.) was coupled with HOBt/DIC (5 equiv. each) (2x45 min), followed by treatments with 20% piperidine in DMF (2x30 min). To control the quality of the linear peptide chain by HPLC and MS, a small portion of the peptidyl resin was treated with TFA/H_2O/TIA/EDT/TIS (90:3:1:3:3; V_{tot} = 100 µl) for about 3 h. Ice-cold diethyl ether was added to precipitate the peptide that was recovered by centrifugation and washed at least three times with ice-cold diethyl ether. The alloc/allyl protecting groups were orthogonally removed by repeated treatments (6x15 min) with $Pd(PPh_3)_4$ (0.5 equiv.) in the presence of $PhSiH_3$ (25 equiv.) in DCM. Side-

chain cyclization was carried out with DIPEA/DEPBT (3:2 equiv.) in DCM/DMF (3:1, v/v) for 72 h. The peptides were cleaved from the resin with TFA/H_2O/TIA/EDT/TIS (90:3:1:3:3; V_{tot} = 1 ml) for about 3 h, precipitated by ice-cold diethyl ether, recovered by centrifugation at 4 °C for 6 min, and washed at least three times with ice-cold diethyl ether. The crude peptides were purified by semipreparative HPLC. The purity (≥ 90%) and identification of the desired peptides were assessed by analytical HPLC and MALDI-TOF-MS (Table S1 and Fig. S1).

Table S1 Analytical characterization of the synthetic peptides used in this work.

Peptide	**$M_{theor.}$[a] (Da)**	**$(M+H)^+_{found}$[b] (Da)**	**t_R[c] (min)**
cyclo-[2,6]-(*Ac*-VKRLQDLQ-NH_2) (**1**)	1021.61	1022.83	28.2
cyclo-[2,6]-(*Ac*-VKRLQDLQY-NH_2) (**1Y**)	1184.68	1185.88	25.9
cyclo-[2,6]-(*FAM*-βAVKRLQDLQY-NH_2) (**FAM-1Y**)	1571.75	1572.77	29.5
Ac-KVEILQHVIDY-NH_2 (**2**)	1396.77	1398.05	27.5
FAM-βAKVEILQHVIDY-NH_2 (**FAM-2**)	1783.85	1784.82	30.2

a. Monoisotopic

b. Measured by MALDI-TOF-MS

c. HPLC gradient: 3% B for 8 min, 3-60% B in 35 min, with A = 0.06% TFA in water and B = 0.05% TFA in CH_3CN

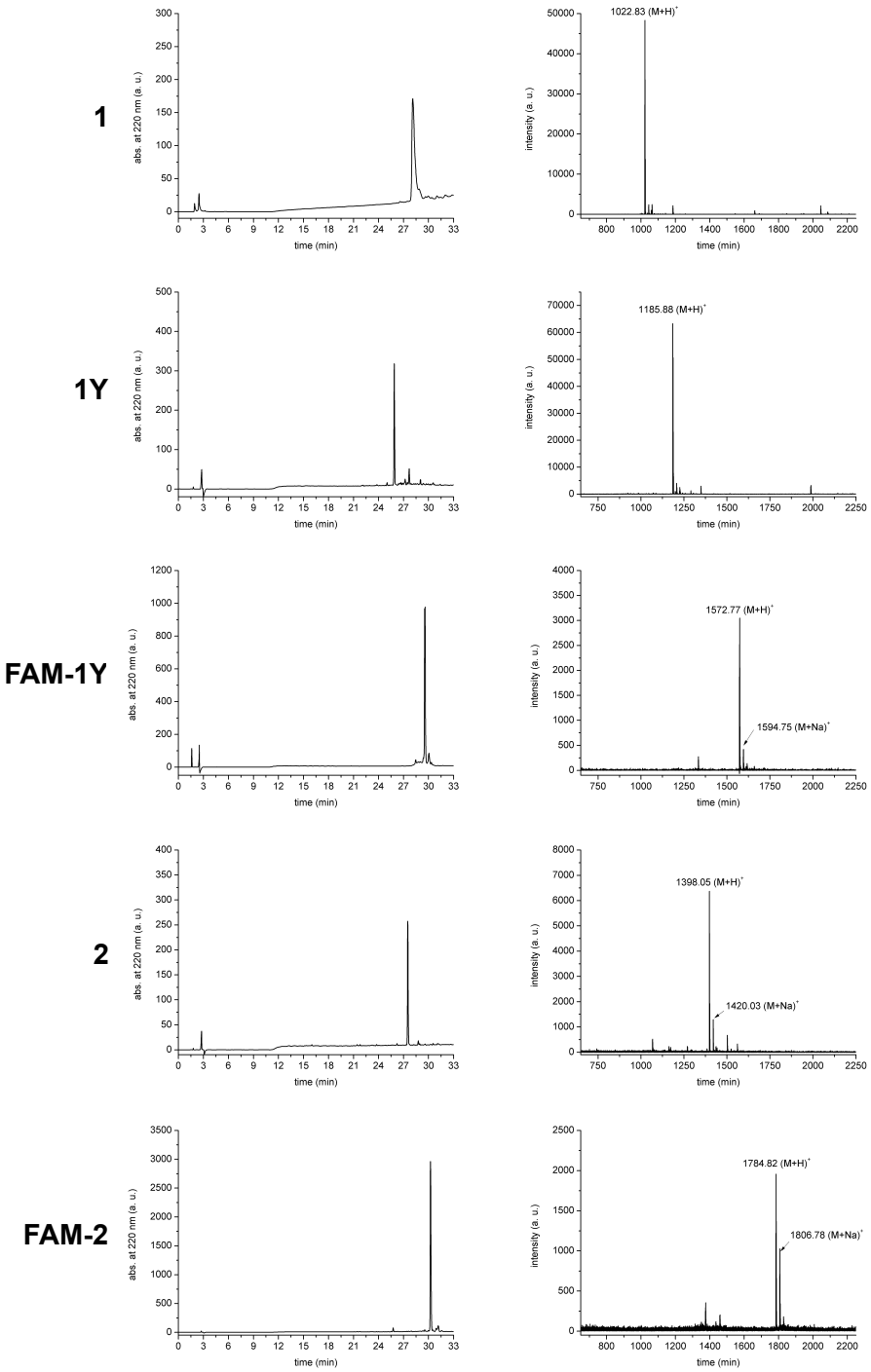

Fig. S1 Analytical HPLC and MALI-TOF-MS of the synthetic peptides used in this work.

3. Protein expression and purification

The cDNA of full-length Id2 (134 residues, ~15 kDa) was inserted into the pET22b(+) expression vector and transformed into the *Echerichia coli* host strain BL21 (DE3). Recombinant inclusion body protein expression was obtained with 1 mM IPTG, followed by incubation at 37 °C for 4 h. Cells were subsequently harvested by centrifugation (4000 rpm, 30 min at 4 °C) and lysed in FastBreak^{TM} cell lysis reagent, including 80 µl 10 mg/ml lysozyme, 4 µl 100 mM PMSF, and 20 µl 1 mg/ml DNase I per 1 g wet cell pellet. To break the disulfide bonds, 100 µl β-mercaptoethanol were added. After 30 min incubation under constant agitation and centrifugation (4000 rpm, 30 min at 4° C), the pellet was washed with wash buffer I (50 mM TRIS-HCl, 10 mM EDTA, 100 mM NaCl, 0.05% triton X-100, pH

8.0). After centrifugation (4000 rpm, 30 min at 4 °C), a second wash step was performed with wash buffer II (50 mM TRIS-HCl, 1 mM EDTA, 100 mM NaCl, pH 8.0). The full-length Id2 protein from the inclusion bodies was solubilized with 8 M urea containing 3% β-mercaptoethanol. The obtained solution was purified via gel filtration chromatography with a Phenomenex BioSep-SEC-s2000 column. The recombinant full-length Id2 protein was characterized by western blot analysis and MALDI-TOF-MS.

4. NMR spectroscopy

All NMR spectra were measured in water (pH ~4) at a peptide concentration of ~1 mM. Initial 1D ^{1}H spectra recorded at temperatures between 278 and 318 K with samples dissolved in H_2O/D_2O (12:1) revealed the best dispersion of signals in the amide region at 303 K. Subsequently 2D NMR spectra were recorded either in H_2O/D_2O (12:1) or D_2O at 303 K. The water signal was suppressed with 3-9-19 WATERGATE. The spin systems of all amino-acid residues were identified using 2D ^{1}H-^{1}H TOCSY spectra (mixing times of 80 and 12 ms) and an additional ^{1}H-^{13}C HSQC spectrum. The sequence-specific assignment was accomplished using phase-sensitive ^{1}H-^{1}H ROESY spectra (mixing time of 200 ms). Spectra were processed using TOPSPIN 3.2 from Bruker. All spectra were referenced to DSS using the standard Bruker sample 2 mM sucrose/0.5 mM DSS at the same temperature and settings. ^{13}C chemical shifts were referenced using a scaling factor Ξ of 0.251449530 according to IUPAC recommendations[3].

5. NMR spectra assignment and distance-constrained molecular modeling

NMR spectra assignment. Complete ^{1}H and ^{13}C resonance assignment was achieved using standard 2D ^{1}H-^{1}H TOCSY, ^{1}H-^{1}H ROESY, ^{1}H-^{13}C HSQC spectra (Fig. S2, S3 and Table S2 for **1** and Fig. S4, S5 and Table S3 for **1Y**). NOE distance restraints were derived from the 2D ROESY spectra. The NOE cross-peaks were classified as very-strong/medium-strong/medium-weak/weak corresponding to applied distance restraints of 2.5/3.5/4.5/5.5 Å. The dihedral angle ranges for ϕ and ψ were predicted from chemical shifts using Talos[4].

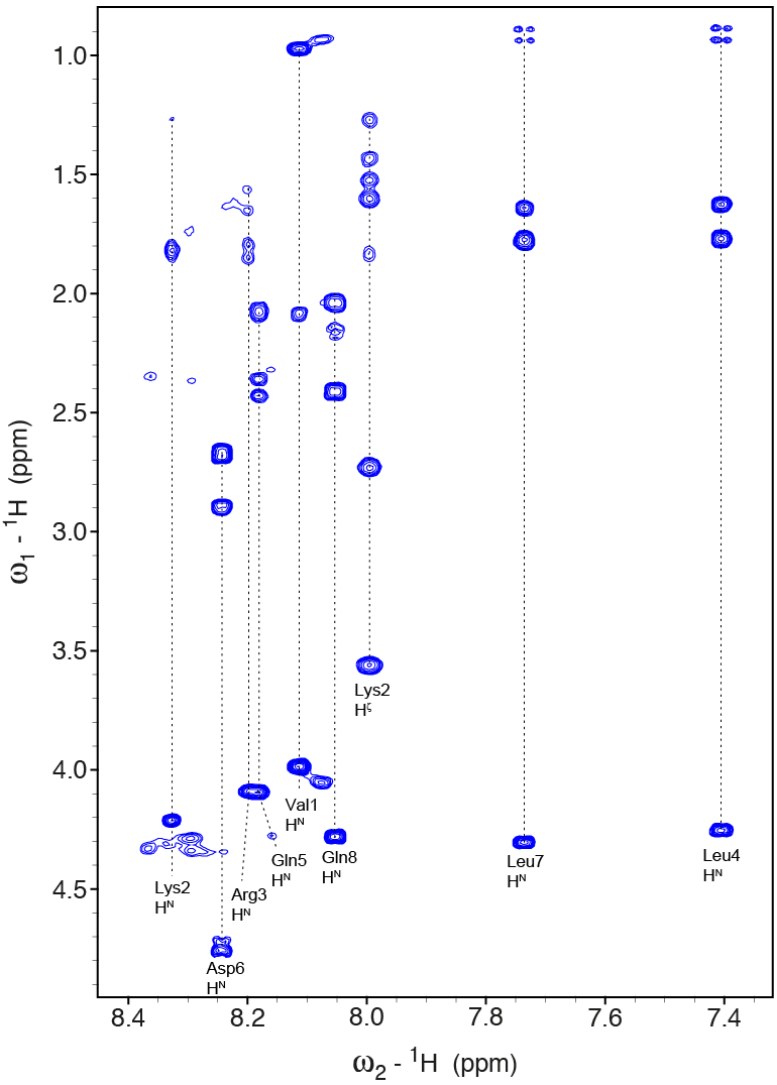

Fig. S2 2D ^{1}H-^{1}H TOCSY spectrum of **1**, ~1 mM in H_2O/D_2O (12:1), at 303 K (mixing time of 80 ms).

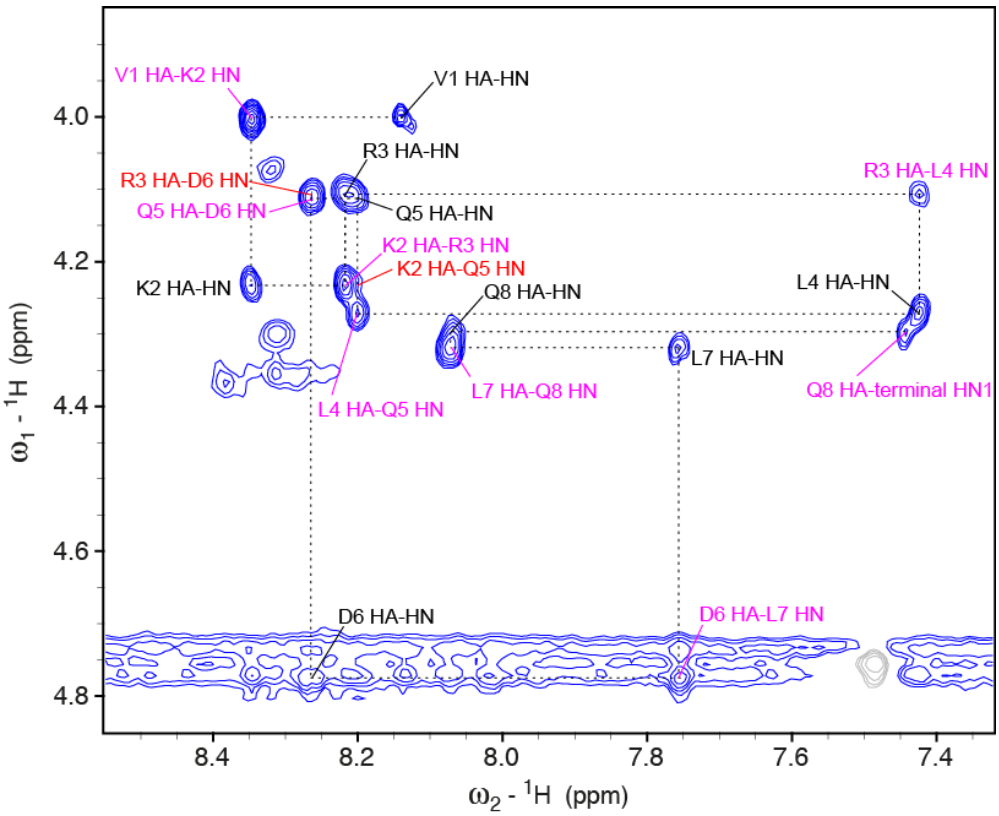

Fig. S3 NMR assignment walk illustrated with a 2D ROESY spectrum of **1**, ~1 mM in H_2O/D_2O (12:1), at 303 K. The region of Hα-HN correlations is shown, blue contours indicate negative signals, grey ones positive signals. Intra-residual Hα-HN correlations are labeled in black and sequential correlations in magenta. The assignment walk is indicated as dotted lines. Possible medium-range correlations are indicated in red.

Table S2 ^{1}H and ^{13}C chemical shifts (ppm) of cyclopeptide **1**, ~1 mM in H_2O/D_2O (12:1) at 303 K.

Residue	α-NH	α-CH	β-CH	γ-CH	δ-CH	ε-CH	ζ-NH (bridge)
V1	8.13	4.00	2.11	0.98/0.99			
		63.3	32.4	21.2/20.6			
K2	8.34	4.23	1.85	1.53/1.28	1.62/1.45	2.74/3.58	8.02
		57.6	31.3	24.7	29.2	41.8	
R3	8.22	4.10	1.87/1.81	1.66/1.59	3.27/3.21	7.28	
		57.7	30.1	27.3	43.0		
L4	7.42	4.26	1.79/1.64	1.63	0.90/0.95		
		56.3	42.2	27.1	23.3/24.9		
Q5	8.20	4.11	2.09	2.44/2.38			
		58.5	28.9	33.9			
D6	8.26	4.75	2.92/2.69				
		53.7	38.5				
L7	7.75	4.32	1.78/1.64	1.77	0.90/0.95		
		55.8	42.2	26.8	23.4/25.0		
Q8	8.07	4.29	2.17/2.05	2.42			
		56.1	29.4	34.0			

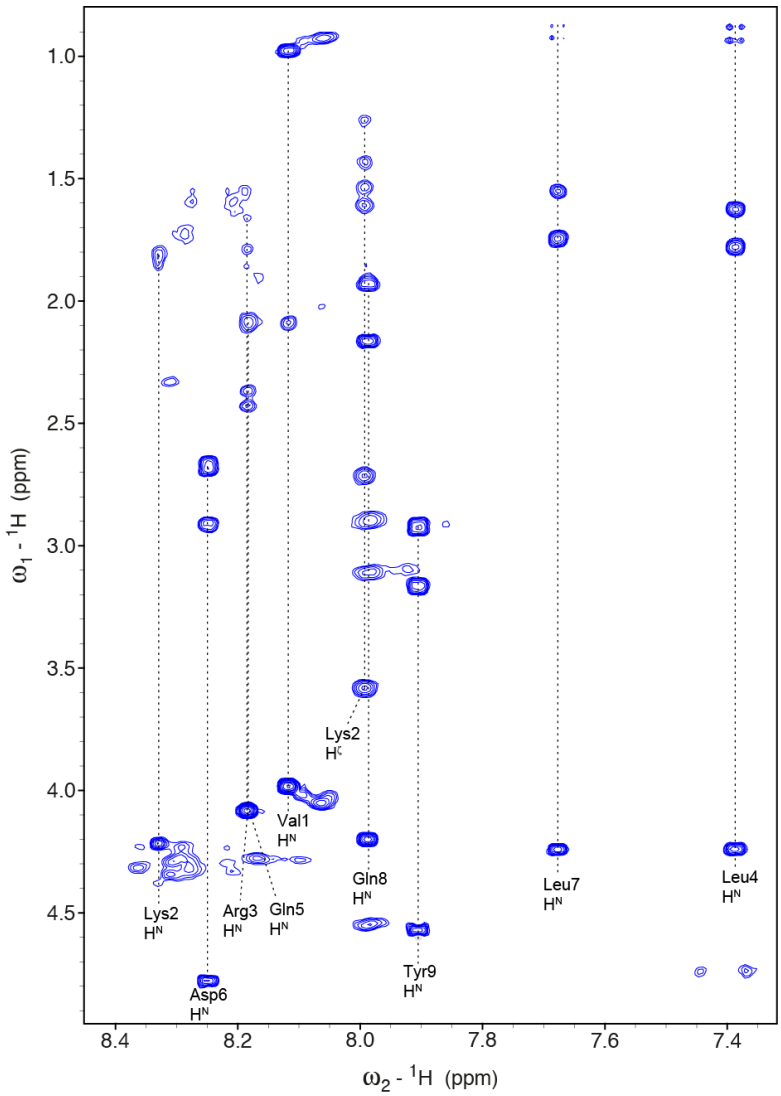

Fig. S4 2D ^{1}H-^{1}H TOCSY spectrum of **1Y**, ~1 mM in H_2O/D_2O (12:1), at 303 K (mixing time of 80 ms).

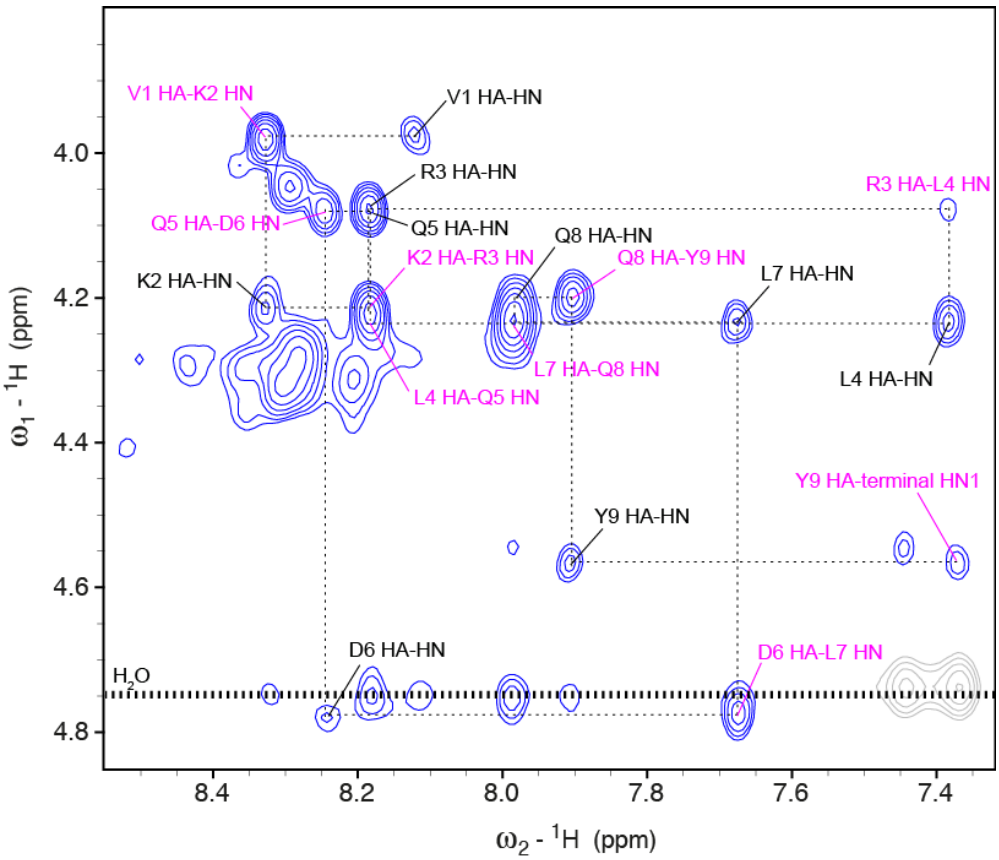

Fig. S5 NMR assignment walk illustrated with a 2D ROESY spectrum of **1Y**, ~1 mM in H_2O/D_2O (12:1), at 303 K. The region of Hα-HN correlations is shown, blue contours indicate negative signals, grey ones positive signals. Intra-residual Hα-HN correlations are labeled in black and sequential correlations in magenta. The assignment walk is indicated as dotted lines.

Table S3 ^{1}H and ^{13}C chemical shifts (ppm) of cyclopeptide **1Y**, ~1 mM in H_2O/D_2O (12:1) at 303 K.

Residue	**α-NH**	**α-CH**	**β-CH**	**γ-CH**	**δ-CH**	**ε-CH**	**ζ-NH (bridge)**
V1	8.11	3.99	2.10	0.98/1.00			
		63.4	32.3	21.2/20.6			
K2	8.33	4.23	1.84	1.55/1.27	1.63/1.45	2.73/3.60	7.99
		57.7	31.2	24.7	29.1	41.8	
R3	8.18	4.09	1.87/1.79	1.58/1.64	3.26/3.19	7.26	
		58.6	30.1	27.2	43.2		
L4	7.39	4.23	1.78/1.64	1.65	0.87/0.94		
		56.3	42.2	27.3	23.4/25.1		
Q5	8.18	4.10	2.09	2.43/2.37			
		57.8	28.9	33.9			
D6	8.25	4.78	2.91/2.69				
		53.8	38.5				
L7	7.68	4.23	1.76/1.56	1.77	0.89/0.92		
		56.3	42.2	26.8	23.3/24.9		
Q8	7.99	4.24	1.94	2.17			
		56.3	29.1	33.5			
Y9	7.91	4.57	3.18/2.92		7.18	6.85	
		57.4	38.7		113.2	118.2	

Structure generation. Cyclopeptides **1** and **1Y** were built up using the Protein Builder and general Builder functions of MOE2015.10[1]. Then, a number of constraints (Tables S4 for **1** and S6 for **1Y**) were applied for the given intramolecular distances on the basis of NMR measurements and the peptide was energy minimized using Amber99 force field as implemented into MOE2015.10. This process led to the α-helical structure of the peptide. Subsequently, the constraints were lifted and the system was re-optimized. Upon optimization, the α-helix as well as the *trans*-configuration of the lactam-bridge was preserved. For the molecular dynamics studies the generated peptide was placed into a 35 Å large cubic box of (explicit) water. The system was slowly heated up from 0 K to room temperature (RT), then equilibrated at RT for 500 ps. The ten lowest-energy structures were superimposed for comparison (Fig. 2 of the manuscript for **1** and Fig. S7 for **1Y**).

Table S4 NOE and dihedral angle constraints of **1** (LYL and ASL are LYS and ASP in the lactam bridge).

NOE type	Residue i	Residue i+n	NOE strength[a]	Upper limit
Sequential	1 VAL HA	2 LYL H	vs	2.50
Intra-residue	1 VAL H	1 VAL QG2	ms	3.50
Intra-residue	2 LYL QB	2 LYL H	ms	3.50
Intra-residue	3 ARG HA	3 ARG H	ms	3.50
Sequential	4 LEU H	5 GLN H	ms	3.50
Intra-residue	4 LEU HB2	4 LEU H	mw	4.50
Intra-residue	3 ARG HB2	3 ARG H	mw	4.50
Sequential	6 ASL HA	7 LEU H	mw	4.50
Sequential	5 GLN HA	6 ASL H	mw	4.50
Intra-residue	5 GLN QB	5 GLN HG2	mw	4.50
Intra-residue	6 ASL HB3	6 ASL H	mw	4.50
Sequential	4 LEU HA	5 GLN H	mw	4.50
Intra-residue	1 VAL H	1 VAL HB	mw	4.50
Intra-residue	5 GLN HA	5 GLN H	mw	4.50
Intra-residue	5 GLN QB	5 GLN H	mw	4.50
Intra-residue	2 LYL H	2 LYL HA	mw	4.50
Intra-residue	4 LEU HA	4 LEU H	mw	4.50
Intra-residue	3 ARG HB3	3 ARG H	mw	4.50
Sequential	2 LYL HE3	6 ASL HD21	mw	4.50
Sequential	2 LYL HA	3 ARG H	mw	4.50
Intra-residue	6 ASL HA	6 ASL H	mw	4.50
Sequential	7 LEU HA	8 GLN H	mw	4.50
Intra-residue	8 GLN H	8 GLN HB3	mw	4.50
Intra-residue	7 LEU H	7 LEU HA	mw	4.50
Intra-residue	4 LEU HB3	4 LEU H	mw	4.50
Sequential	2 LYL HG3	6 ASL HD21	mw	4.50
Sequential	6 ASL H	7 LEU H	mw	4.50
Intra-residue	5 GLN HG2	5 GLN H	mw	4.50
Sequential	1 VAL H	2 LYL H	mw	4.50
Sequential	5 GLN H	6 ASL H	mw	4.50
Intra-residue	8 GLN H	8 GLN QG	w	5.50
Intra-residue	5 GLN HG3	5 GLN H	w	5.50
Sequential	2 LYL HD2	6 ASL HD21	w	5.50
Sequential	2 LYL HD3	6 ASL HD21	w	5.50
2 LYL (ϕ, ψ)	-82.0 to -42.0	-54.4 to -14.1		
3 ARG (ϕ, ψ)	-84.9 to -44.9	-54.5 to -14.5		
4 LEU (ϕ, ψ)	-84.5 to -44.5	-67.3 to -8.5		
5 GLN (ϕ, ψ)	-86.7 to -46.7	-52,9 to -12,9		
6 ASL (ϕ, ψ)	-115.8 to -61.1	-41.0 to 36.1		

[a] The NOE strengths were classified into weak (w), medium weak (mw), medium strong (ms) and very strong (vs)

Table S5 NMR-derived structure parameters for **1**.

Parameter	Value/Number
NOE constraints	34
intraresidue	20
interresidue	14
Dihedral angles constraints	10
NOE constraints below upper limits	
very-strong/medium-strong/medium-weak/weak (2.5/3.5/4.5/5.5 Å)	34
Dihedral angles violations >5°	0
Force field energies (kJ/mol)	
total	-3.0145 E+04
van der Waals	7.3029 E+03
electrostatic	-2.9955 E+05
RMSD to the mean coordinates (Å) all atoms	1.266
Cα atoms (residues 1-8) (Å)	0.526
Cα and Cβ atoms (residues 1-8) (Å)	0.660

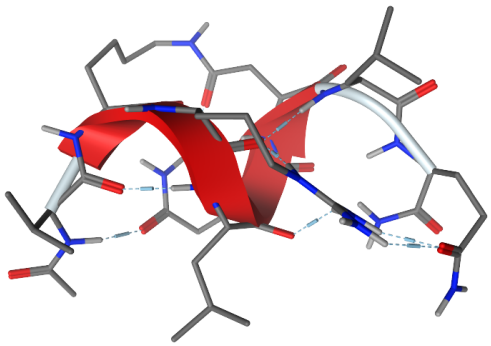

Fig. S6 One of the ten lowest energy NMR-derived structures of cyclo-[2,6]-(Ac-VKRLQDLQ-NH_2) (**1**). Backbone H-bonds: CO(V1)–HN(L4) (1.98 Å), CO(K2)–HN(D6) (2.68 Å), and CO(R3)–HN(L7) (2.07 Å).

Table S6 NOE and dihedral angle constraints of **1Y** (LYL and ASL are LYS and ASP in the lactam bridge).

NOE type	Residue i	Residue i+n	NOE strength[a]	Upper limit
Intra-residue	7 LEU H	7 LEU HA	3.50	ms
Intra-residue	1 VAL H	1 VAL QG2	3.50	ms
Intra-residue	4 LEU HA	4 LEU H	3.50	ms
Intra-residue	2 LYL H	2 LYL HA	3.50	ms
Intra-residue	6 ASL HB3	6 ASL H	3.50	ms
Sequential	2 LYL HE2	6 ASL HD21	3.50	ms
Intra-residue	6 ASL HA	6 ASL H	4.50	mw
Intra-residue	8 GLN H	8 GLN QG	4.50	mw
Intra-residue	4 LEU HB2	4 LEU H	4.50	mw
Sequential	8 GLN HA	9 TYR H	4.50	mw
Intra-residue	4 LEU HB3	4 LEU H	4.50	mw
Intra-residue	8 GLN H	8 GLN QB	4.50	mw
Sequential	1 VAL HA	2 LYL H	4.50	mw
Intra-residue	1 VAL H	1 VAL HB	4.50	mw
Intra-residue	2 LYL QB	2 LYL H	4.50	mw
Sequential	6 ASL HA	7 LEU H	4.50	mw
Intra-residue	5 GLN QB	5 GLN HG2	4.50	mw
Sequential	6 ASL H	7 LEU H	4.50	mw
Sequential	7 LEU H	8 GLN H	4.50	mw
Sequential	7 LEU HA	8 GLN H	5.50	w
Sequential	2 LYL HD2	6 ASL HD21	5.50	w
Sequential	2 LYL HD3	6 ASL HD21	5.50	w
Sequential	2 LYL HG2	6 ASL HD21	5.50	w
Sequential	2 LYL HG3	6 ASL HD21	5.50	w
Sequential	3 ARG HA	4 LEU H	5.50	w
Sequential	1 VAL H	2 LYL H	5.50	w
2 LYL (ϕ, ψ)	-85.0 to -45.0	-57.3 to -6.2		
3 ARG (ϕ, ψ)	-86.1 to -46.1	-58.0 to -18.0		
4 LEU (ϕ, ψ)	-85.0 to -45.0	-66.5 to -4.3		
5 GLN (ϕ, ψ)	-82.8 to -42.8	-54.1 to -14.1		
6 ASL (ϕ, ψ)	-116.4 to -46.5	-46.9 to 7.9		

[a] The NOE strengths were classified into weak (w), medium weak (mw) and medium strong (ms)

Table S7 NMR-derived structure parameters for **1Y**.

Parameter	Value/Number
NOE constraints	26
intraresidue	13
interresidue	13
Dihedral angles constraints	10
NOE constraints below upper limits	
medium-strong/medium-weak/weak (3.5/4.5/5.5 Å)	26
Dihedral angles violations >5°	0
Force field energies (kJ/mol)	
total	-3.54604 E+04
van der Waals	8.68479 E+03
electrostatic	-3.45126 E+05
RMSD to the mean coordinates (Å) all atoms	0.670
Cα atoms (residues 1-9) (Å)	0.411
Cα and Cβ atoms (residues 1-9) (Å)	0.469

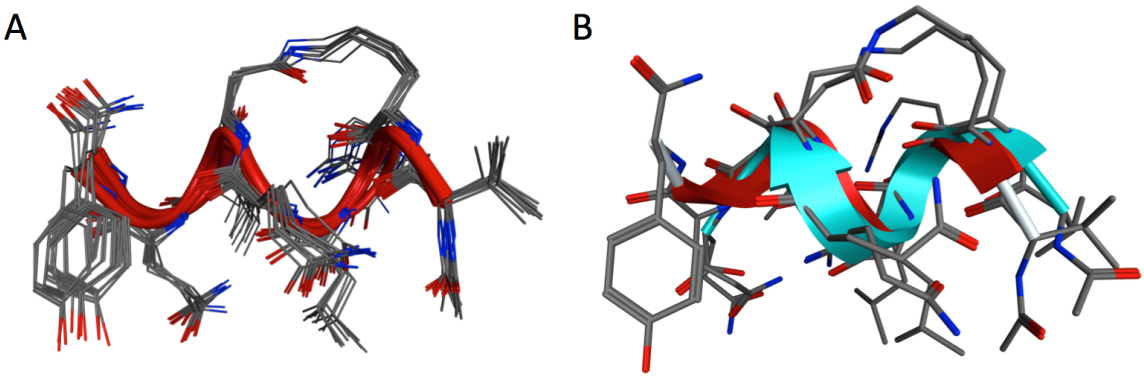

Fig. S7 NMR-derived structure of cyclo-[2,6]-(Ac-VKRLQDLQY-NH_2) (**1Y**). (A) Superposition of the ten lowest energy structures from the molecular dynamics simulation. (B) Superposition of two lowest energy NMR-derived structures of **1** (cyan-colored ribbon) and **1Y** (red-colored ribbon). Backbone H-bonds for **1Y**: CO(V1)–HN(Q5) (1.93 Å), CO(K2)–HN(D6) (1.87 Å), CO(L4)–HN(L7) (2.38 Å), CO(L4)–HN(Q8) (2.10 Å) and CO(Q5)–HN(Y9) (2.39 Å).

6. Superposition of the crystal structure of the Id2 HLH homodimer (PDB ID: 4AYA) with the solution NMR structure of the Id3 HLH homodimer (PDB ID: 2LFH)

Fig. S8 Superposition of the crystal structure of the parallel four-helix bundle of the Id2 HLH homodimer (PDB ID: 4AYA, yellow) with the solution NMR structure of the Id3 HLH homodimer (PDB ID: 2LFH, 20 lowest energy structures in red).

7. Superposition of the helix of cyclopeptide 1 with helix-1 or helix-2 from the crystal structure of the Id2 HLH homodimer (PDB ID: 4AYA)

For the superposition with the native helices of Id2 the coordinates of helix-1 and helix-2 were separately extracted from the crystal structure (PDB ID: 4AYA). Then, the Cα atoms of each amino acid of cyclopeptide **1** were fitted to the corresponding Cα atoms within the helix (Table S8 and Fig. S9). To generate the ligand interactions, the given helix (helix-1 or helix-2) was first removed from the 4AYA structure, the fitted coordinates of the peptide were placed into the complex and the system was optimized (using MOE2015.10). The desired ligand interaction maps were generated by the Ligand Interaction function of MOE2015.10 (Fig. S10).

Table S8 Hydrophobic three-residue patterns present in cyclopeptide **1** and in helix-1 and helix-2 of the Id proteins (based on the sequence of Id2. See Fig. 1a for comparison with the sequences of the other Id proteins).

Helix	**Hydrophobic pattern**			**RMSD (Å) of Cα superposition with 1**	**Distance (Å) between Cβ of**		
	i	**i+3**	**i+6**		**i and Nα-V1**	**i+3 and Cβ-L4**	**i+6 and Cβ-L7**
1	**V1**	**L4**	**L7**	--	--	--	--
Helix-1	L36	M39	C42	1.38	0.64	1.41	2.03
Helix-1	Y43	L46	L49	1.26	1.13	1.48	1.36
Helix-2	M62	L65	V68	1.20	0.57	1.59	1.44
Helix-2	L65	V68	Y71	1.13	0.83	1.23	1.02

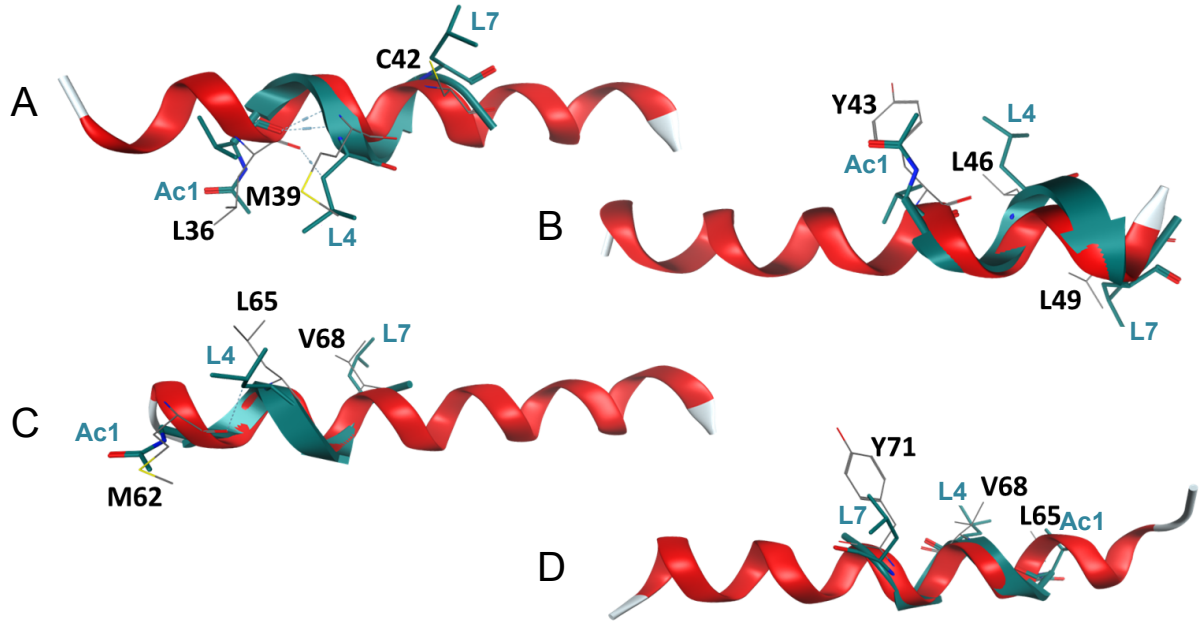

Fig. S9 Superposition of one representative structure of cyclo-[2,6]-(Ac-VKRLQDLQ-NH_2) (**1**) with each of the hydrophobic three-residue patterns reported in Table S8 for helix-1 and helix-2 (PDB ID: 4AYA). The hydrophobic three-residue pattern is shown (in teal for **1**, in grey for the helix in the crystal structure).

A Superposition of 1 with helix-1 (L36, M39, C42)

Interactions of 1 with		
Helix-2	**Helix-2'**	**Helix-1'**
K61	K61	Y43
I64	M62	
L65	L65	
V68	Q66	
	V68	
	I69	

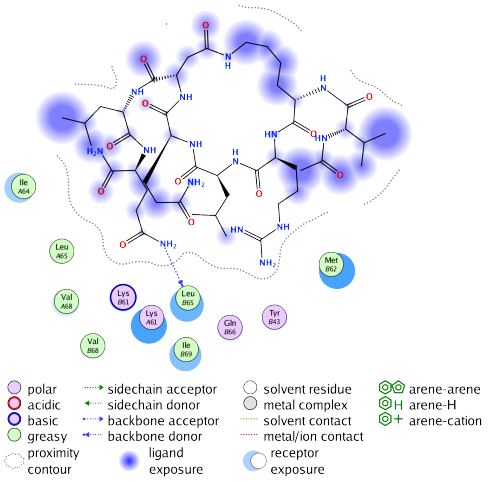

B Superposition of 1 with helix-1 (Y43, L46, L49)

Interactions of 1 with		
Helix-2	**Helix-2'**	**Loop**
I64	L65	P51
H67	V68	S52
V68	I69	I53
Y71	I72	P54
	L73	Q55
	Q76	

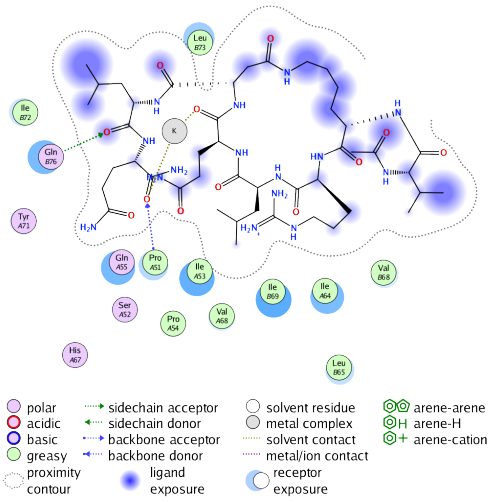

C Superposition of 1 with helix-2 (M62, L65, V68)

Interactions of 1 with			
Helix-1	**Helix-2'**	**Helix-1'**	**Loop**
Y43	Y71	L36	S52
V50	I72	Y37	I53
L65		N38	
V68		M39	
		C42	
		Y43	
		K45	
		L46	
		L49	
		V50	

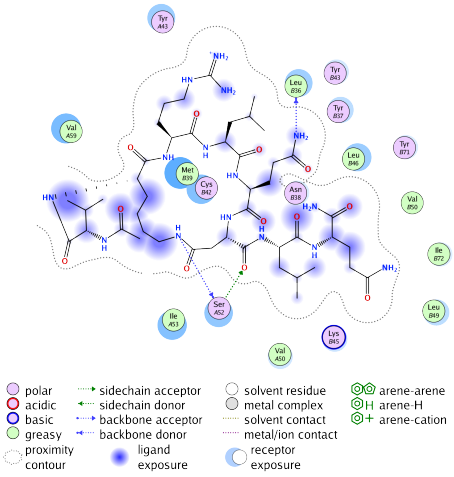

D Superposition of 1 with helix-2 (L65, V68, Y71)

Interactions of 1 with		
Helix-1	**Helix-2'**	**Helix-1'**
Y43	L65	L35
L46	V68	L36
V50	Y71	M39
	I72	C42
	L75	Y43
		L46

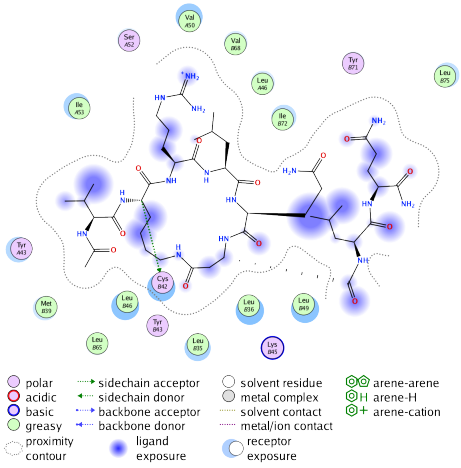

Fig. S10 Ligand interaction map of the energy-minimized complex of cyclopeptide **1** and the parallel four-helix bundle of Id2 (PDB ID: 4AYA). The four models (A-D) were obtained by superposition of cyclopeptide **1** with each of the relevant hydrophobic three-residue patterns reported in Table S8, followed by removal of the given helix (helix-1 or helix-2) and subsequent energy minimization (force field Amber99 as implemented into MOE 2015.10).

8. Binding studies by SAW biosensor technology

The protein was immobilized with the offline coating tool from NanoTemper. A mixture of 12.5 µl Oxyma Pure (400 mM in 10 mM PBS, pH 7.4) and 12.5 µl DIC (100 mM in 10 mM PBS, pH 7.4) was added on each channel for 10 min to activate the carboxylic groups of the dextran chip. This step was repeated three times. After removal of the activation solutions from the surface by aspiration, the protein solution (30 µM in 10 mM NaOAc buffer) was pipetted on the layer. The coupling step was repeated twice (2x40 min). Before removing the protein solution, 3.5 µl of 10% trehalose in 10 mM NaOAc buffer were added. The chip was washed with 1% trehalose five times after aspiration of the solution from the channels. To cap the remaining activated carboxylic groups of the dextrane chip, a mixture of 2 M ethanolamine in 10 mM NaOAc buffer was given onto the coated surface for 10 min. Five min before removing the capping solution, 3.5 µl of 10% trehalose were added. The chip was washed again with 1% trehalose five times after aspiration of the solution. Finally, the chip was dried under nitrogen. The peptides with increasing concentrations were dissolved in running buffer (NaOAc buffer, pH 4.5) and injected into a constant buffer flow of 40 µl/min. The data points from at least four independent experiments were fitted by using the Hill equation supported by the program OriginPro.

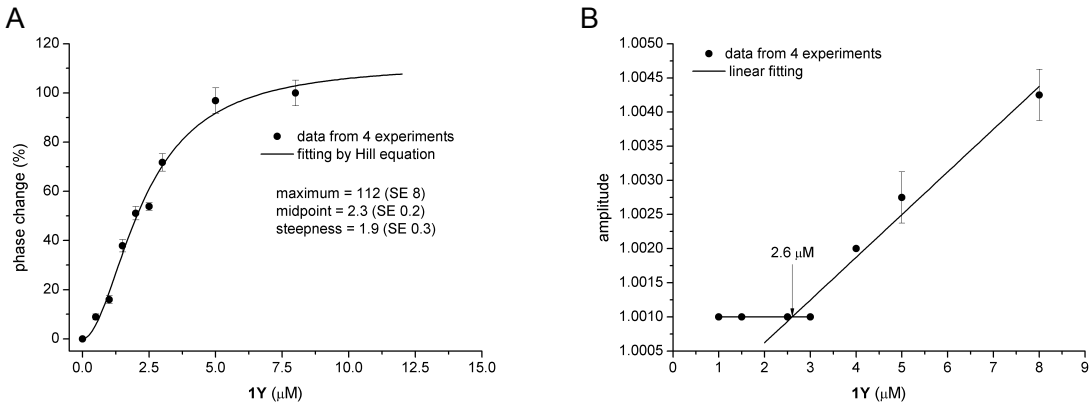

Fig. S11 Titration of immobilized Id2 with **1Y** ($K_{0.5}$ = 2.3 ± 0.2). (A) Phase and (B) amplitude (viscoelasticity) change.

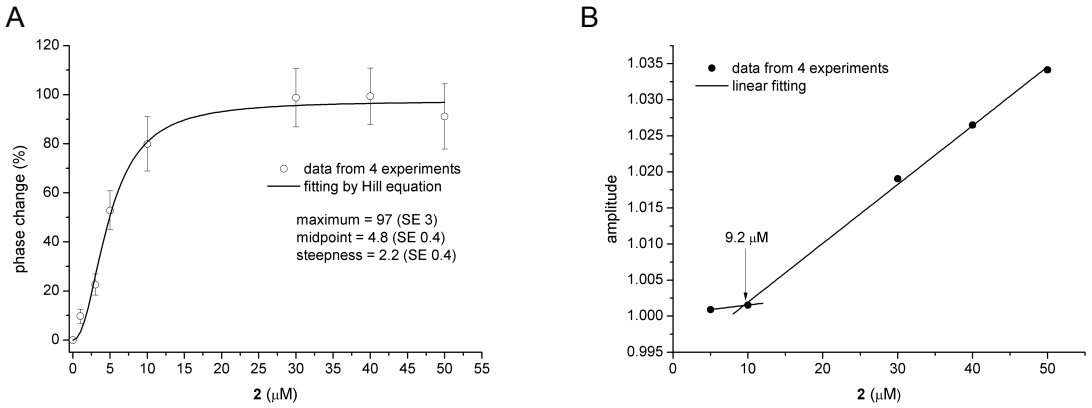

Fig. S12 Titration of immobilized Id2 with **2** ($K_{0.5}$ = 4.8 ± 0.4). (A) Phase and (B) amplitude (viscoelasticity) change.

9. Peptide stability in cell culture medium

FAM-1Y or **FAM-2** were dissolved in DMEM containing 5% FBS and 1% penicillin-streptomycin and incubated at 37 °C under constant shaking. At the indicated time points, an aliquot was taken and examined by MALDI-TOF-MS. Additionally, the peptides were checked by analytical HPLC using a C-18 column and detected at 220 nm as well as 440 nm.

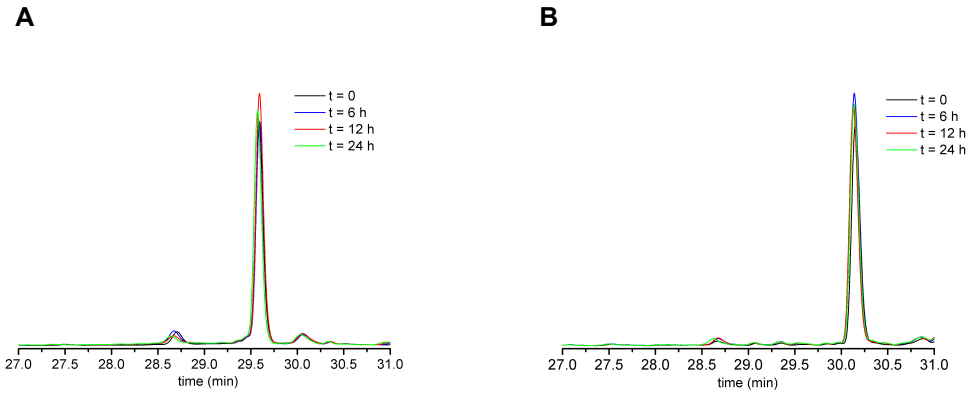

Fig. S13 HPLC profiles of (A) **FAM-1Y** and **FAM-2** (B) in DMEM medium with 5% FBS and 1% penicillin-streptomycin at different time points (incubation temperature: 37 °C), detected at 220 nm. The peak area does not change with time.

10. Peptide stability in human blood serum and in the presence of trypsin

For a stability assay in human blood serum (taken from a healthy volunteer), stock solutions of **FAM-1Y** and **FAM-2** in DMSO were diluted to 150 µM with the serum (the final DMSO amount was 1%) and incubated at 37 °C under constant agitation. At the indicated time points, a 30 µl aliquot was taken, treated with 60 µl of the mixture H_2O/CH_3CN/EtOH/TFA (7:1:1:1, v/v), incubated at 4 °C for 4 h and centrifuged. The supernatant was analyzed by MALDI-TOF-MS and analytical HPLC using a C-18 column and UV-detection at 220 nm and 480 nm.

For a stability assay in the presence of trypsin, stock solutions of **FAM-1Y** and **FAM-2** in DMSO were diluted to 150 µM with a solution of trypsin in 0.1 M ammonium bicarbonate (the peptide/trypsin ratio was 1000:1 and the final DMSO amount was 1 %) and incubated under constant agitation at 37 °C. At the indicated time points, a 40 µl aliquot was taken, treated with 20 µl of 10 % TFA to stop the digestion and checked by MALDI-TOF-MS and analytical HPLC using a C-18 column and UV-detection at 220 nm and 480 nm.

The amount of **FAM-1Y** in human blood serum decreased during the investigated time window of 6 h, with a half-life of around 4 h (Fig. S14A). In contrast, the amount of **FAM-2** did not change significantly (Fig. S14B). We assumed that this might have been due to the propensity of **2** to self-associate. Therefore, we compared the sensitivity of **FAM-1Y** and **FAM-**2 towards proteases: indeed, limited proteolysis can be useful to assess the accessibility of cleavage sites to proteases as well as the degree of backbone flexibility[5-7]. As **FAM-1Y** and **FAM-2** contain the basic residues R3 and K1, respectively, we used trypsin in a peptide/protease ratio of 1000:1. Under these conditions, **FAM-1Y** was fast hydrolyzed at the cleavage site R3-L4 (Fig. S14C), whereas **FAM-2** remained stable during the investigated time window of 6 h, as shown by the comparison of the HPLC profiles at the beginning and after 6 h of treatment with trypsin (Fig. S14D). We investigated the propensity of **2** to self-associate also by CD spectroscopy: the CD spectra in water were concentration-dependent and suggested the presence of β-sheets (Fig. S14E). However, in the presence of 30% TFE, a secondary structure-stabilizing and membrane environment-mimicking solvent[8], the peptide showed a helix-like CD signature, however with moderate intensity, suggesting self-association (Fig. S14F).

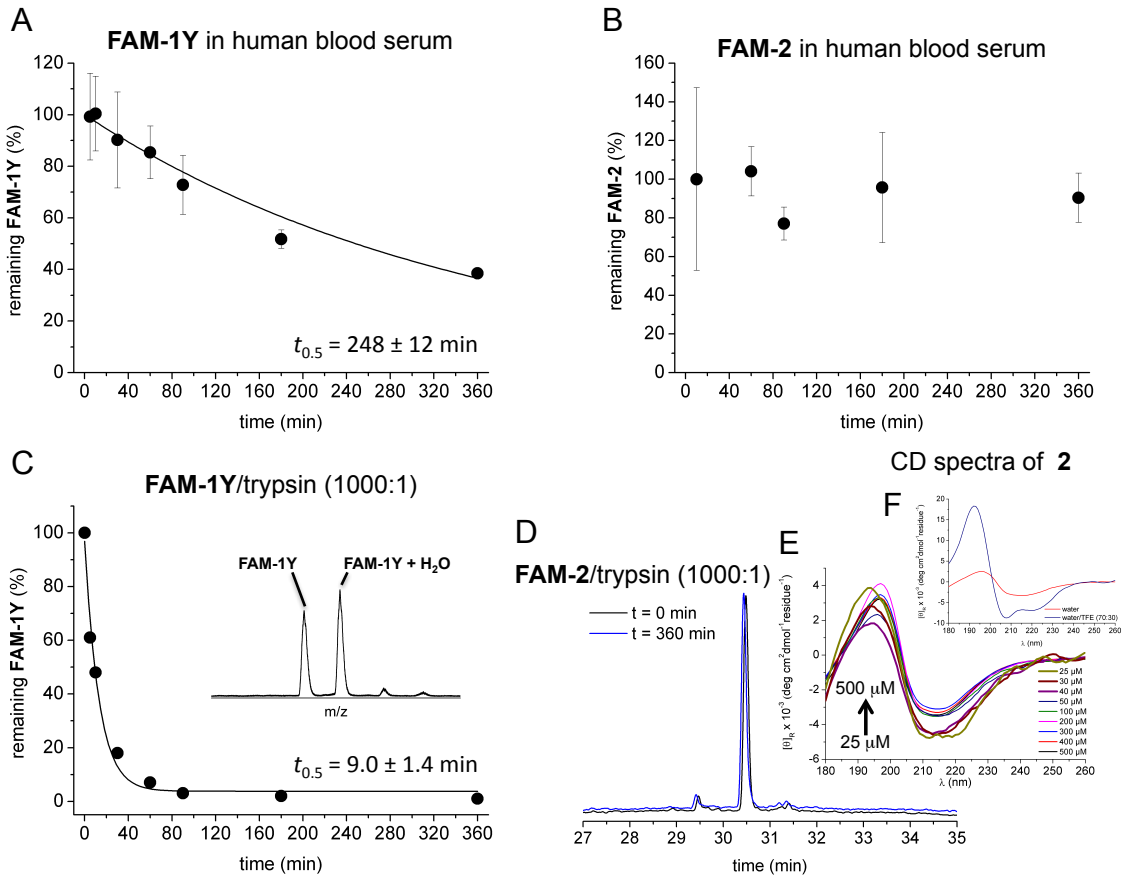

Fig. S14 Stability of **FAM-1Y** and **FAM-2** in human blood serum and in the presence of trypsin at 37 °C over a time window of 6 h. (A, B) Stability of **FAM-1Y** (A) and **FAM-2** (B) in human blood serum over 360 min at 37 °C (the graphs show the mean values ± SD of four and two independent experiments, respectively). (C) Trypsin digestion of **FAM-1Y**, as obtained by the area percentage of the HPLC peaks of **FAM-1Y** and its hydrolyzed product (-R3-*OH H*-L4-). The two MS peaks are shown in the inset (the graph shows the mean values ± SD of two independent experiments). (D) HPLC profile of **FAM-2** in the presence of trypsin at 0 min and 360 min (detection at 480 nm). (E, F) CD spectra of **2** in water over the concentration range of 25-500 µM (E), and comparison of the CD spectra of **2** (50 µM) in water (red curve) and in the presence of 30% TFE (blue curve).

11. Cellular uptake of FAM-1Y and FAM-2

The breast cancer cell lines MCF-7 and T47D were grown in DMEM-high glucose and the bladder cancer cell line T24 in RPMI-1640, with 10% FBS, 1% L-glutamine and 1% penicillin-streptomycin at 37 °C and 5% CO_2. To investigate the peptide uptake, $3x10^5$ cells were seeded on cover glasses. After 24 h, the medium was exchanged for medium with 5% FBS containing either 10 µM **FAM-1Y** or **FAM-2**, and the cells were incubated for 8 h, 12 h, 16 h and 24 h in the dark. To determine the cellular uptake and localization, cells were counterstained with Hoechst-33342 1:2000 (10 mg/ml in water) and incubated for 15 min at 37 °C in the dark. To remove excess FAM-peptides and Hoechst dye, cells were washed with PBS twice. Fluorescence microscopy was carried out on an Olympus IX70 inverted microscope and analyzed with the Cell F software.

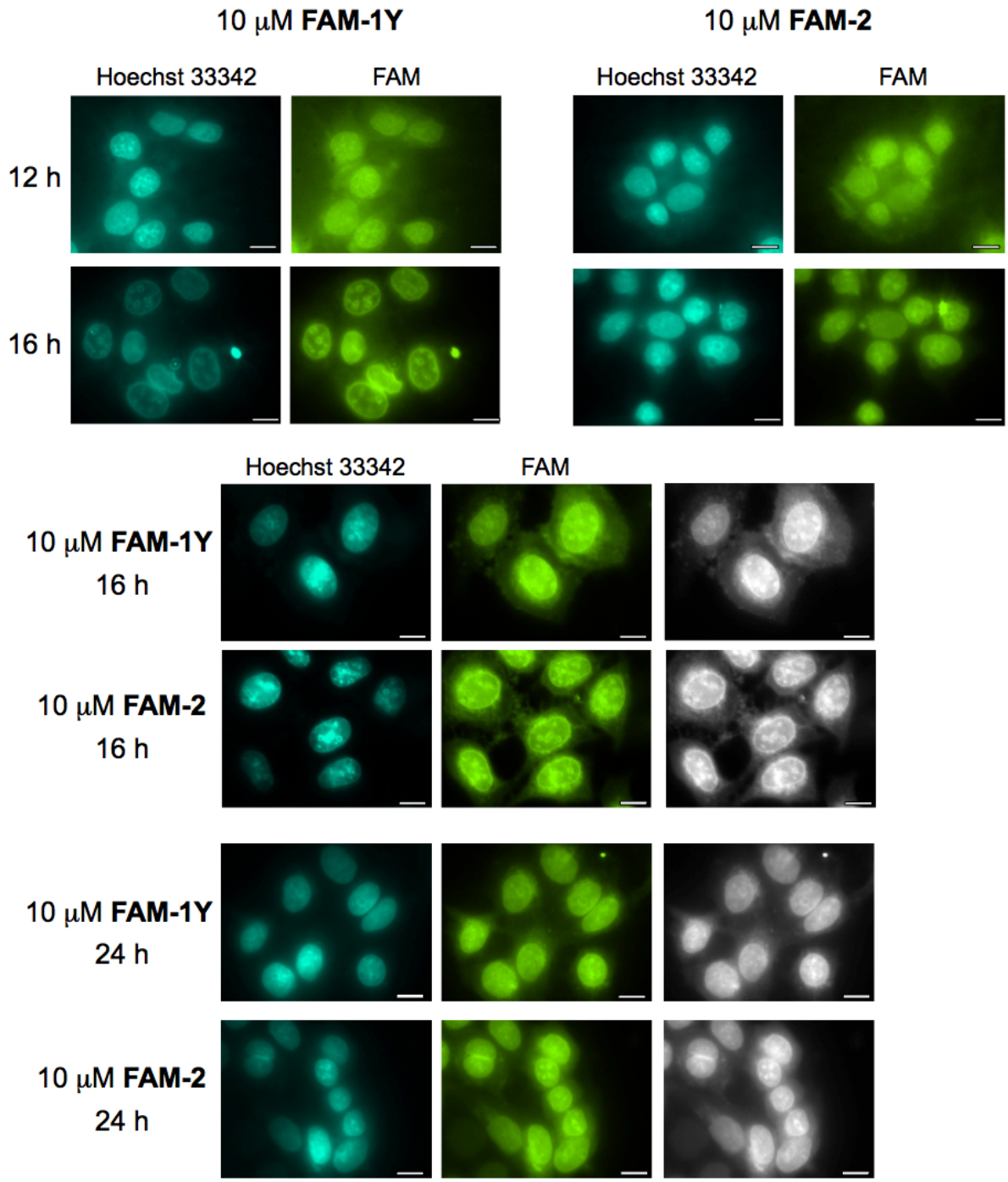

Fig. S15 Uptake of the fluorescence-labeled peptides **FAM-1Y** and **FAM-2** into MCF-7 cells. Fluorescence microscopy images were taken after incubation with each peptide at a concentration of 10 μM for the indicated times. Nuclei were stained with Hoechst 33342 nucleic acid stain and are visible in cyan (scale bar: 10 μm).

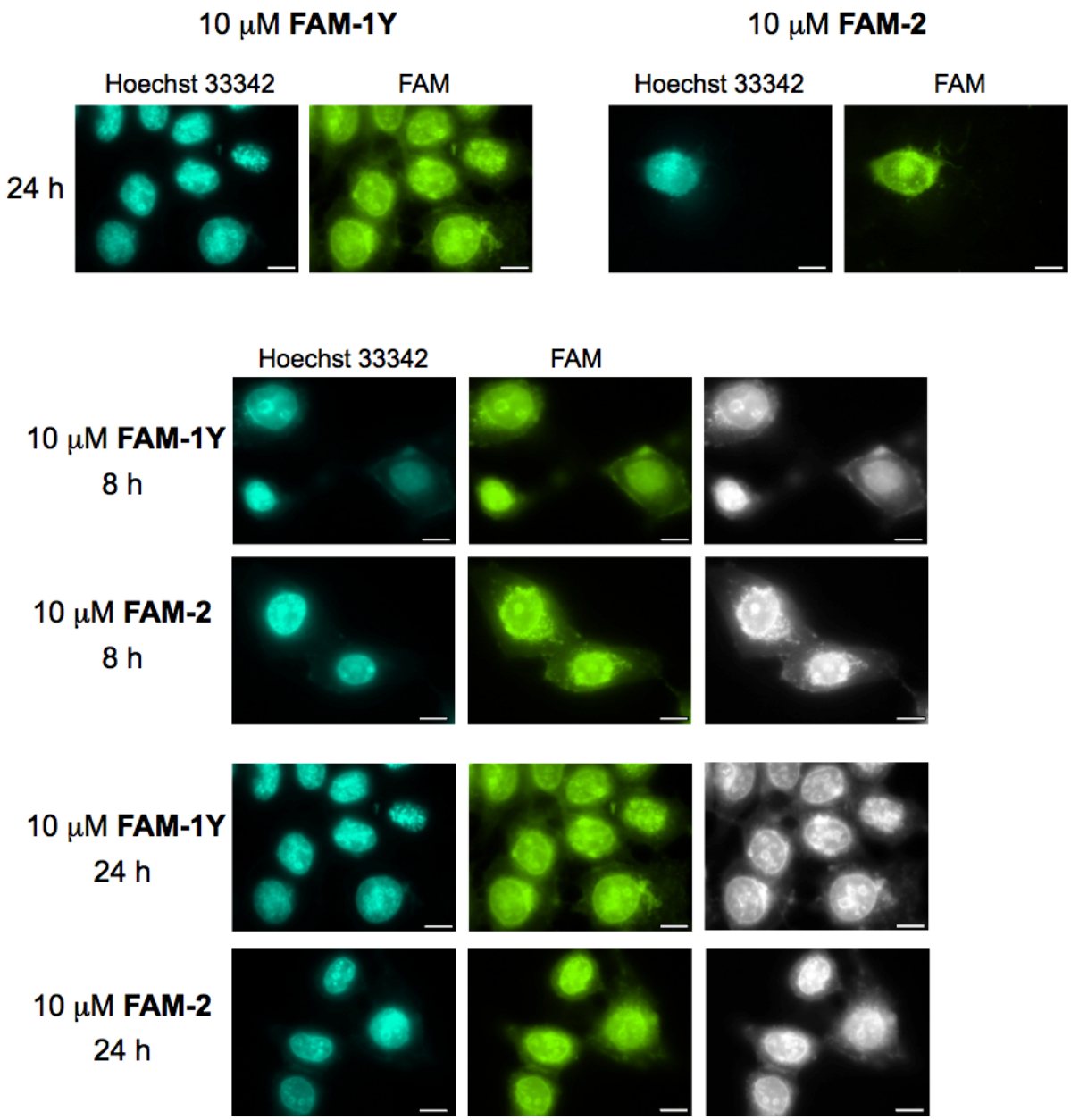

Fig. S16 Uptake of the fluorescence-labeled peptides **FAM-1Y** and **FAM-2** into T47D cells. Fluorescence microscopy images were taken after incubation with each peptide at a concentration of 10 μM for the indicated times. Nuclei were stained with Hoechst 33342 nucleic acid stain and are visible in cyan (scale bar: 10 μm).

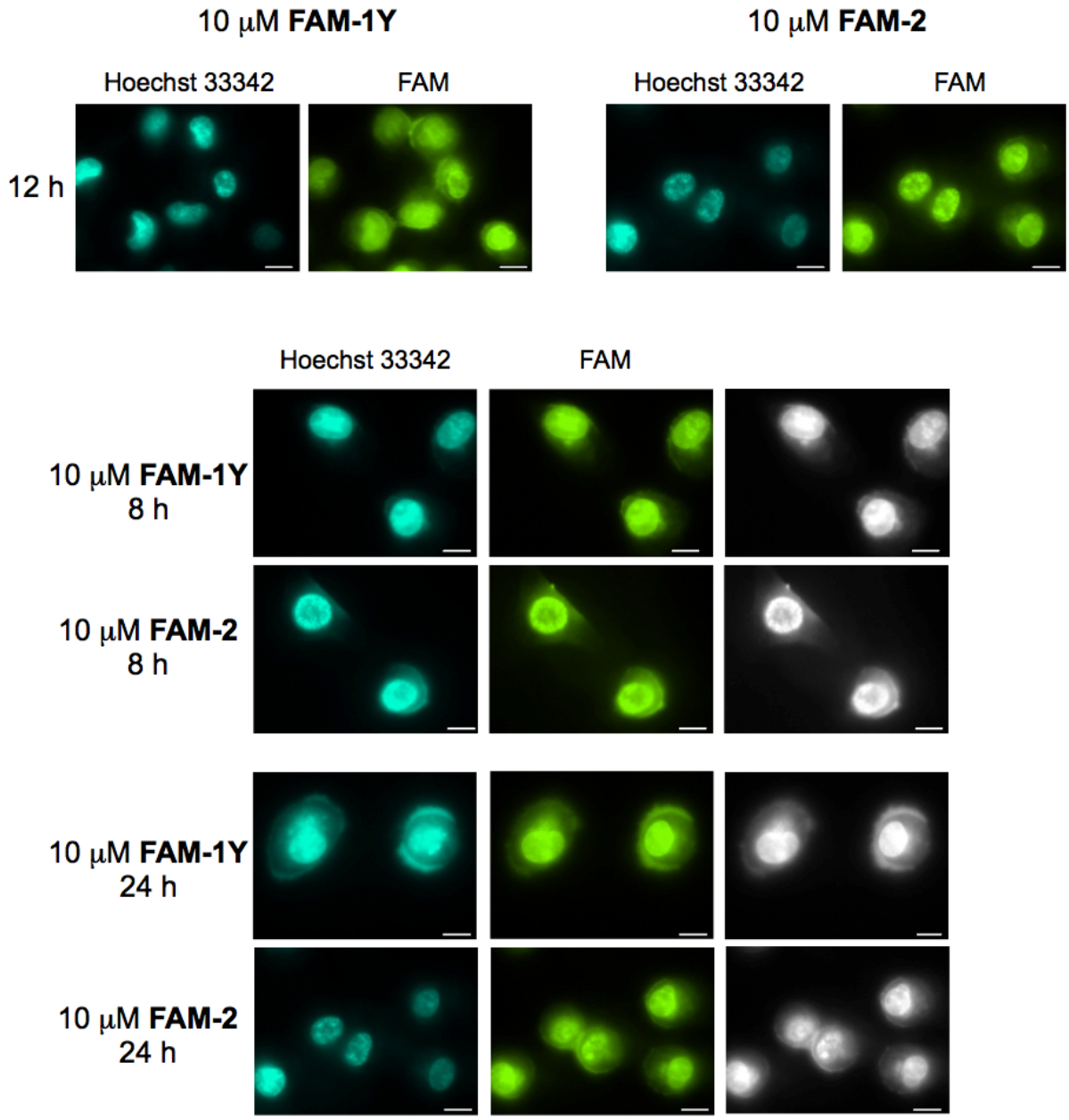

Fig. S17 Uptake of the fluorescence-labeled peptides **FAM-1Y** and **FAM-2** into T24 cells. Fluorescence microscopy images were taken after incubation with each peptide at a concentration of 10 μM for the indicated times. Nuclei were stained with Hoechst 33342 nucleic acid stain and are visible in cyan (scale bar: 10 μm).

12. Time- and temperature-dependent cellular uptake of FAM-1Y and FAM-2

Cells of the breast cancer cell line MCF-7 were grown in DMEM with 10% FBS at 37 °C and 5% CO_2. To investigate the peptide uptake, $5x10^5$ cells were seeded into 35 mm tissue culture dishes. After 24 h, the medium was exchanged for medium without FBS containing either 10 μM **FAM-1Y** or **FAM-2**, and the cells were incubated for 4 h and 8 h in the dark at 4 °C and 37 °C. To remove excess FAM-peptides, cells were washed with PBS twice. Cellular uptake of the labeled peptides was analyzed by detection of FAM fluorescence using flow cytometry.

Upon incubation at 37 °C, only a minor fraction of cells was found to contain **FAM-1Y** after 4 h, whereas the majority of cells treated with **FAM-2** already displayed FAM fluorescence. However, after 8 h at 37 °C, all cells were found to contain **FAM-1Y**. Thus, the cellular uptake of the cyclopeptide was significantly slower than that of the linear peptide at 37 °C. Upon incubation at 4 °C

for 8 h, no FAM-positive cells were detected for both **FAM-1Y** and **FAM-2**. This experiment suggests that the cellular uptake of the two peptides at the concentration of 10 μM is more likely to occur via energy-dependent endocytotic pathways, which are all simultaneously blocked at 4°C, rather than via energy-independent passive diffusion. However, this does not exclude the possibility that passive diffusion might take place at higher peptide concentrations. Besides **FAM-1Y** and **FAM-2**, we also tested fluorescence-labeled hexaarginine, **FAM-R_6** (5(6)-carboxyfluorescein-βA-R_6-amide), as representative of a cell-penetrating peptide (CPP)[9]. This peptide was prepared by solid-phase methodology, as described above for the other synthetic peptides used in this work (MALDI-TOF-MS: $M_{theor.}$ 1383.56, M_{found} for $M+H^+$ 1384.94. HPLC: t_R 21.6 min, 90% pure). Upon incubation with 10 μM **FAM-R_6** at 37 °C, all cells were found to contain hexaarginine after 4 h; however, longer incubation (8 h) significantly decreased the percentage of cells containing this peptide. As CPPs are able to enter cells very fast, their cellular uptake is generally investigated over a narrow time window (0.5-2 h). However, a few examples of time-dependent cellular uptake of CPPs are reported in the literature showing that the accumulation of CPPs in cells may decrease after having reached a maximum[10]. Again, after 8 h incubation with 10 μM **FAM-R_6** at 4 °C, no cells containing hexaarginine were detected. Further studies will be necessary to fully characterize the transport mechanism of **FAM-1Y** and **FAM-2** and to compare it with other classes of CPPs (amphipatic, hydrophobic, cationic), although the uptake mechanisms of CPPs (direct penetration, endocytosis, formation of inverted micelles) are still debated and appear to strongly depend on the CPP sequence and concentration, on the experimental protocols, on the cargo as well as on the cell type[11].

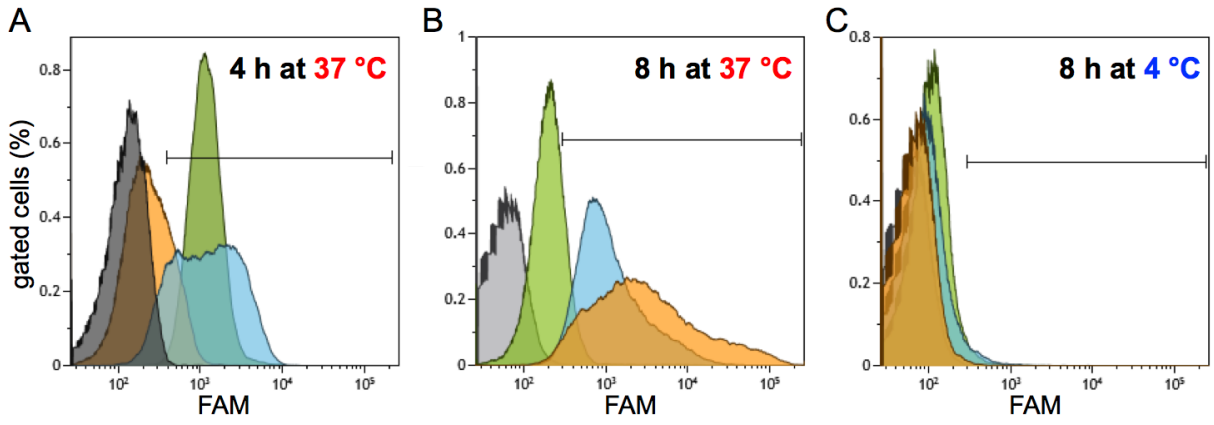

	FAM-positive cells (%)		
untreated			
FAM-2	**87**	**98**	**3**
FAM-1Y	**23**	**97**	**0**
FAM-R_6	**100**	**19**	**2**

Fig. S18 Time- and temperature-dependent uptake of the fluorescence-labeled peptides **FAM-1Y** and **FAM-2** into MCF-7 cells. The latter were incubated with 10 μM of each peptide at the temperature and for the incubation time indicated. The cells were detached with an Accutase® solution, washed and analyzed by flow cytometry. Cells were gated on live cells, and untreated cells were used to determine the FAM-negative population. (A, B) Incubation at 37 °C for 4 h (A) and 8 h (B). (C) Incubation at 4 °C for 8 h. **FAM-R_6** (10 μM) has been used for comparison.

13. Viability assay of peptide-treated cancer cells

To determine the inhibitory effect of each peptide on cell viability, the MTT assay was used. Cells ($1x10^4$/well) in medium containing 10% FBS were seeded into 96-well culture plates. The day after, cells were treated with various concentrations of each peptide in 100 μl medium containing 5% FBS as triplicates for 8 h, 18 h and 24 h. To determine the cell viability, 10 μl 5 mg/ml MTT solution were added to the peptide-treated and non-treated cells for 2 h at 37 °C in the dark. Then the medium was aspirated, cells were lysed with 100 μl DMSO and the absorbance of the resulting product formazan

was measured at 550 nm with a Tecan Infinite M200 Pro reader. The data points from three independent experiments were fitted by using the program OriginPro; the dose response curves gave the following values for the minima and maxima: **1Y** at MCF-7 cells: 52±2% and 94±1%; **2** at MCF-7 cells: 65±1% and 95±1%; **1Y** at T47D cells: 49±1% and 104±3%; **2** at T47D cells: 60±2% and 96±1%; **1Y** at T24 cells: 49±3% and 96±2%; **2** at T24 cells: 44±5% and 90±1% (Fig. 5 of the manuscript).

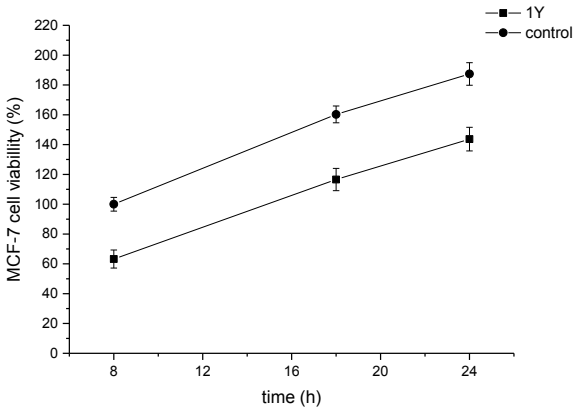

Fig. S19 MCF-7 viability after 8 h, 18 h and 24 h treatment with 100 µM cyclopeptide **1Y**. Cell viability was assessed using the MTT assay. The graph shows the mean values ± SD of three independent experiments, and the viability of untreated MCF-7 cells at 8 h was set to 100%.

14. Viability assay of peptide-treated primary human lung fibroblasts

As a control for non-cancer cells, and to exclude general cytotoxic effects of the peptides, primary human lung fibroblasts were used, as they contain very low Id-protein levels in comparison to the investigated cancer cells. Cells ($1x10^4$/well) in complete growth medium (DMEM, 10% FBS, 1% penicillin/streptomycin, 1% L-glutamine, 1% non-essential amino acids) were seeded into 96-well culture plates. The day after, cells were treated with various concentrations of each peptide in 100 µl medium containing 5% FBS as triplicates for 24 h. To determine the cell viability, 10 µl 5 mg/ml MTT solution were added to the peptide-treated and non-treated cells for 1 h at 37 °C in the dark. The medium was aspirated, cells were lysed with 100 µl DMSO and the absorbance of the resulting product formazan was measured at 550 nm with a Tecan Infinite M200 Pro reader. The data points from three independent experiments are shown in Fig. S20. No relevant changes in viability of the primary human lung fibroblasts up to a concentration of 1 mM of both peptides were observed.

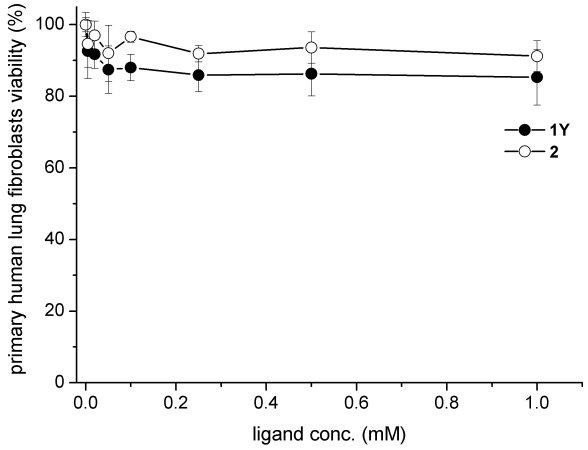

Fig. S20 Effect of **1Y** and **2** on primary human lung fibroblasts viability. Viability of the cells treated with cyclopeptide **1Y** or the linear Id helix-2 fragment **2** for 24 h was determined by the MTT assay. The graph represents the mean value ± SD of three independent experiments.

15. Propidium iodide (PI) staining for cell cycle analysis

Cells ($5x10^5$ cells) were grown in 35 mm cell culture dishes with 1.5 ml medium containing 10% FBS for 24 h. The day after, cells were incubated for additional 8 h, 18 h or 24 h in the presence of 100 µM peptide (**1Y** or **2**) in medium containing 5% FBS. Afterwards, the supernatant was harvested and transferred into 1.5 ml Eppendorf tubes. The cells were detached with 500 µl Accutase® solution and centrifuged. After removal of the supernatant the cell pellet was resuspended in 200 µl PBS. For fixation, 2 ml of ice-cold 70% ethanol was added drop-wise to the suspension under gentle agitation. After freezing for at least 1 h at -20 °C, the cell suspension was centrifuged and washed twice with PBS. The cells were then stained with a solution of 25 µl 0.4 mg/ml propidium iodide, 25 µl 1 mg/ml RNase and 450 µl PBS. After incubation for 15 min at 37 °C in the dark, the fluorescence of propidium iodide bound to DNA was measured with the BD FACSCanto II flow cytometer. Cell cycle analyses from three independent experiments were performed with the Kaluza 1.5a flow cytometer software.

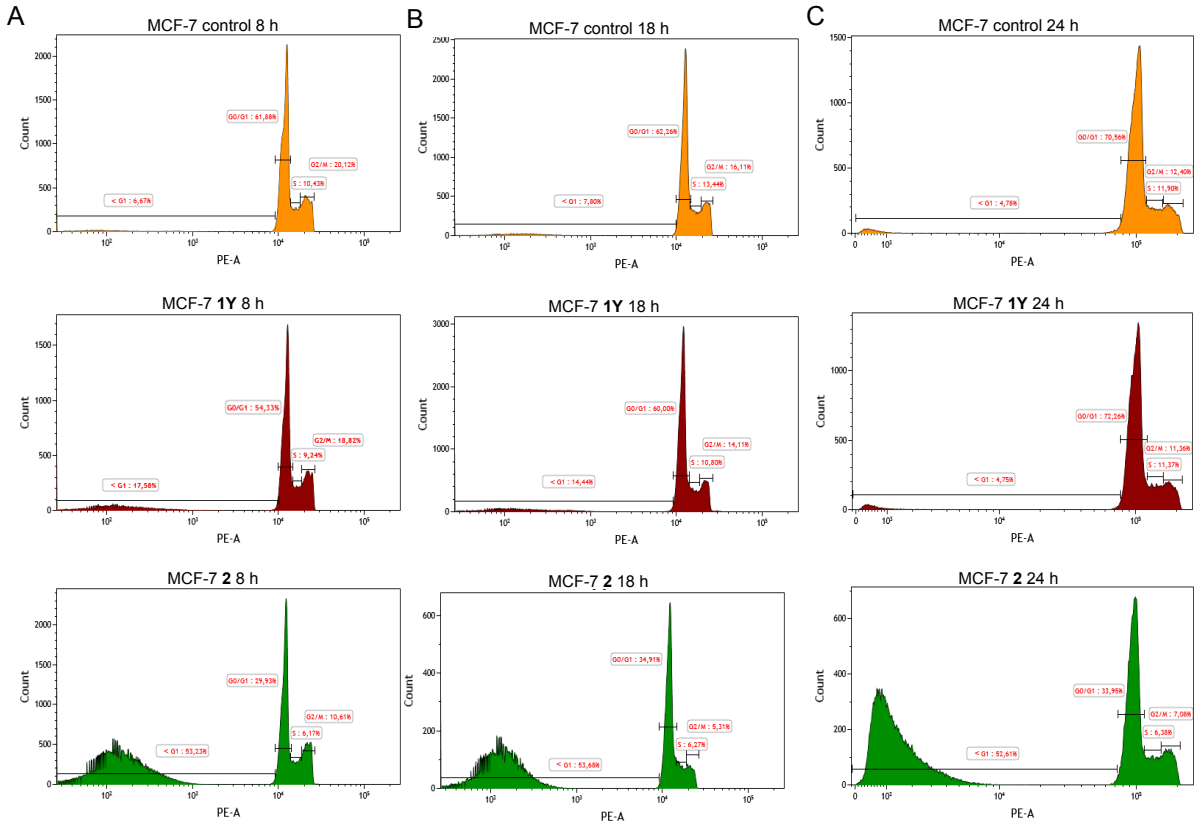

Fig. S21 Cell cycle analysis of MCF-7 cells. One representative experiment is shown: (A) 8 h, (B) 18 h and (C) 24 h incubation with 100 µM **1Y** or 100 µM **2**, compared to the control.

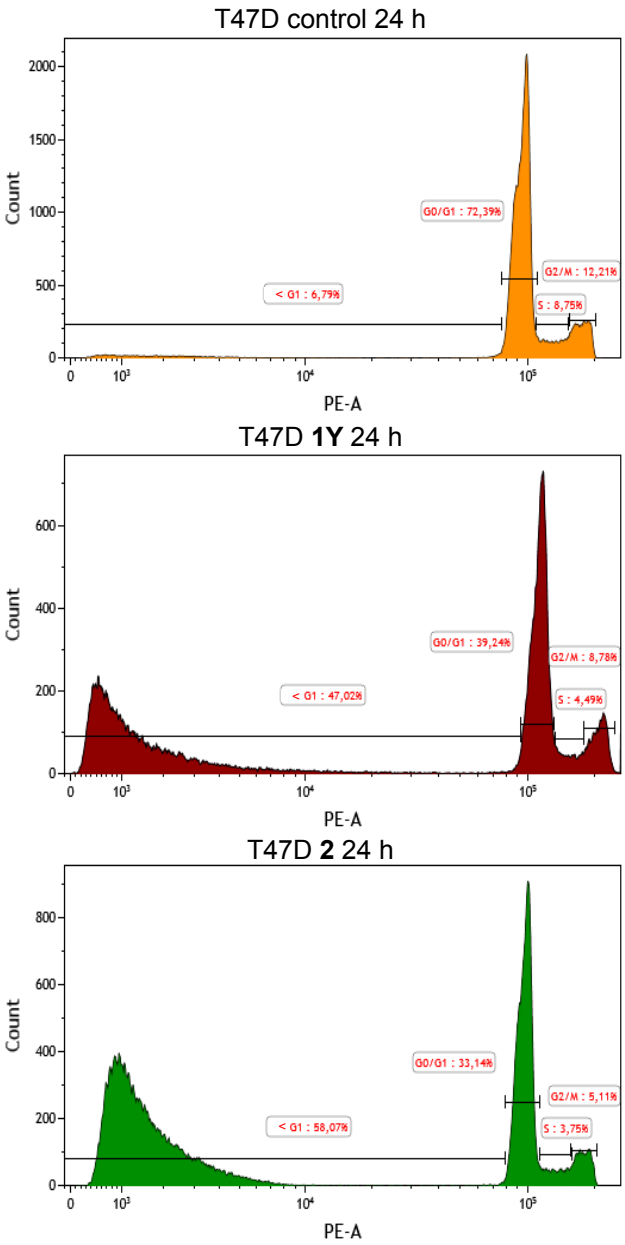

Fig. S22 Cell cycle analysis of T47D cells. One representative experiment is shown for 24 h incubation with 100 µM **1Y** or **2**, compared to the control.

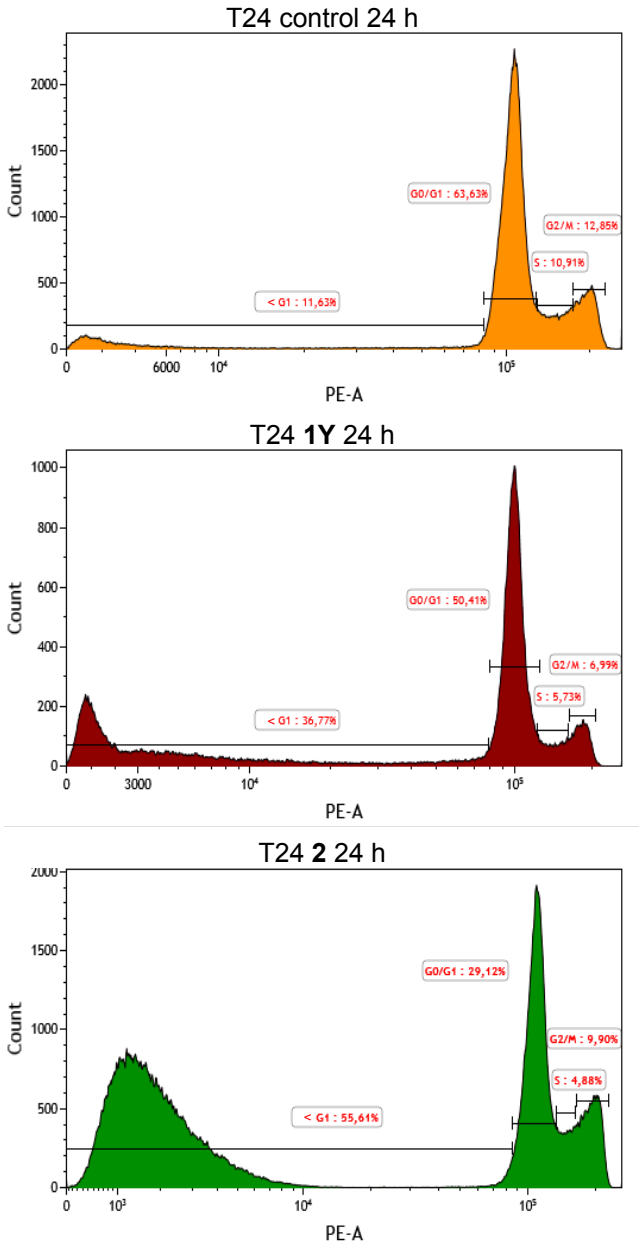

Fig. S23 Cell cycle analysis of T24 cells. One representative experiment is shown for 24 h incubation with 100 µM **1Y** or **2**, compared to the control.

Table S9 Comparison of the cell cycle phases of MCF-7 cells with and without treatment with 100 µM **1Y** for 8 h, 18 h and 24 h. Values represent percentages determined in Fig. S21, which were recalculated after omission of the $<G_0/G_1$ fraction. No significant differences between the untreated and treated cells could be detected at any incubation time.

	8 h			**18 h**			**24 h**		
	G_0/G_1 (%)	**S (%)**	**G_2/M (%)**	**G_0/G_1 (%)**	**S (%)**	**G_2/M (%)**	**G_0/G_1 (%)**	**S (%)**	**G_2/M (%)**
control	66.2±8.5	12.6±2.7	21.0±3.4	68.9±7.8	15.1±1.8	16.0±2.3	71.4±4.9	15.6±3.6	13.0±4.2
1Y	63.2±8.5	16.7±2.6	20.0±2.1	70.8±7.0	12.7±2.9	16.5±1.5	71.1±13.6	15.4±2.9	13.5±3.2

16. CFSE staining for proliferation analysis

For the proliferation assay, MCF-7 cells ($5x10^5$ cells) were washed twice with 2 ml PBS to get rid of the medium. The cell pellet was resuspended in 110 µl PBS with 10 µM CFSE and incubated for 10 min at 37 °C in the dark. To remove any remaining dye, 2 ml DMEM containing 10% FBS were added, incubated for additional 5 min at 37 °C and washed twice with 2 ml PBS. The cells were resuspended in 1.5 ml DMEM containing 10% FBS and seeded into 35 mm cell culture dishes. The day after, cells were incubated for 24 h in the presence of 100 µM peptide (**1Y**) or without peptide as a control. After detachment with 500 µl Accutase® solution, the cells were washed twice with 2 ml PBS and resuspended in 100 µl PBS. The fluorescence intensity of CFSE was measured with the BD FACSCanto II flow cytometer and analyses from three independent experiments were performed with the Kaluza 1.5a flow cytometer software.

17. Apoptosis/necrosis assay

MCF-7 cells ($5x10^5$ cells) were grown in 35 mm cell culture dishes with 1.5 ml medium containing 10% FBS for 24 h. The day after, cells were incubated for 8 h or 24 h in the presence of 100 µM peptide **1Y** in medium containing 5% FBS. Cells were then stained with $DiOC_6$ (50 nM final concentration) for 15 min in the dark at 37 °C. The supernatant was harvested and transferred into 1.5 ml Eppendorf tubes. The cells were detached with 500 µl Accutase® solution, collected and centrifuged. After removal of the supernatant, the cells were washed with 1% FBS/PBS solution. Subsequently, the cells were resuspended in a staining solution containing 25 µl 0.4 mg/ml propidium iodide and 475 µl 1% FBS/PBS. After incubation for 15 min on ice in the dark, the fluorescence signals of propidium iodide and $DiOC_6$ were measured with the BD FACSCanto II flow cytometer. The analyses from two independent experiments were performed with the Kaluza 1.5a flow cytometer software.

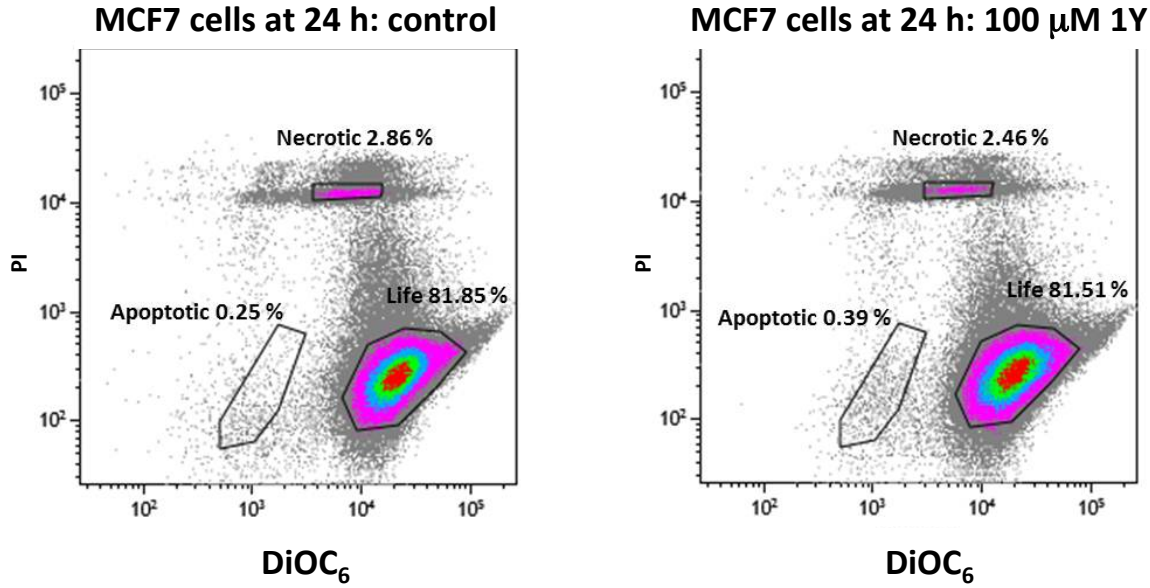

Fig. S24 Cytotoxic effect of **1Y** (100 µM) on MCF-7 cells after 24 h treatment, as measured by flow cytometry. After treatment, cells were exposed to the dye $DiOC_6$ and the DNA/RNA intercalating dye propidium iodide (PI) to detect, respectively, apoptotic cells (reduced mitochondrial membrane potential, low $DiOC_6$ staining) and necrotic cells (no plasma membrane integrity, high PI staining).

18. References

[1] Molecular Operating Environment (MOE), *Chemical Computing Group Inc., 1010 Sherbooke St. West, Suite #910, Montreal, QC, Canada, H3A 2R7* **2016**.

[2] M. Valiev, E. J. Bylaska, N. Govind, K. Kowalski, T. P. Straatsma, H. J. J. van Dam, D. Wang, J. Nieplocha, E. Apra, T. L. Windus, W. A. de Jong, *Comput. Phys. Commun.* **2010**, *181*, 1477-1489.

[3] J. L. Markley, A. Bax, Y. Arata, C. W. Hilbers, R. Kaptein, B. D. Sykes, P. E. Wright, K. Wüthrich, *Pure Appl. Chem.* **1988**, *70*, 117-142.

[4] Y. Shen, F. Delaglio, G. Cornilescu, A. Bax, *J. Biomol. NMR* **2009**, *44*, 213-223.

[5] A. Fontana, P. P. de Laureto, B. Spolaore, E. Frare, P. Picotti, M. Zambonin, *Acta Biochim. Pol.* **2004**, *51*, 299-321.

[6] S. J. Hubbard, F. Eisenmenger, J. M. Thornton, *Protein Sci.* **1994**, *3*, 757-768.

[7] M. J. Suskiewicz, J. L. Sussman, I. Silman, Y. Shaul, *Protein Sci.* **2011**, *20*, 1285-1297.

[8] K. R. Wang, B. Z. Zhang, W. Zhang, J. X. Yan, J. Li, R. Wang, *Peptides* **2008**, *29*, 963-968.

[9] G. Tunnemann, G. Ter-Avetisyan, R. M. Martin, M. Stockl, A. Herrmann, M. C. Cardoso, *J. Peptide Sci.* **2008**, *14*, 469-476.

[10] H. Yamashita, T. Kato, M. Oba, T. Misawa, T. Hattori, N. Ohoka, M. Tanaka, M. Naito, M. Kurihara, Y. Demizu, *Sci. Rep.* **2016**, *6*, 33003.

[11] Z. Guo, H. Peng, J. Kang, D. Sun, *Biomed. Rep.* **2016**, *4*, 528-534.